The Autocorrelation Function and Doppler Spectral Moments: Geometric and Asymptotic Interpretations

RICHARD E. PASSARELLI, JR. AND ALAN D. SIGGIA[1]

Massachusetts Institute of Technology, Department of Earth, Atmospheric and Planetary Science, Cambridge, MA 02139

(Manuscript received 17 February 1983, in final form 15 July 1983)

ABSTRACT

The relationships between the Doppler spectrum of velocities and the autocorrelation function can be studied via simple geometric and power series expansion relations. The asymptotic expansion of the autocorrelation function in terms of the central moments of the Doppler spectrum provides a new theoretical framework for time-domain spectral moment estimation and illustrates the trade-offs in optimal moment estimation. A number of new moment estimators are derived via this general approach and evaluations of three new spectral width estimators demonstrate that the implementation of a single spectral width estimator is generally not the best approach.

1. Introduction

One of the most challenging problems in science is to make a complete extraction of information from a signal. A corollary problem that confronts radar meteorologists is the extraction of "essential" information from an overwhelming signal. The ability of a pulsed Doppler radar to generate of order 10^6 numbers per second has forced the development of a variety of data compression techniques, the most widely used being autocorrelation estimators for the mean and variance of the Doppler spectrum (see Zrnic', 1979, for a review of Doppler spectral moment estimation). The development of the so-called pulse-pair mean velocity algorithm (Rummler, 1968; see also Miller and Rochwarger, 1972) was an important factor in the rapid expansion of Doppler radar meteorology in the 1970's, since it provided an accurate estimate of the spectral mean which could be implemented economically in real-time with the existing technology.

Recently, Siggia (1981) presented a real-time Doppler spectral analyzer that transforms the radar time series to the frequency domain, manipulates the Doppler spectrum to reject ground clutter and estimates certain spectral properties. During the course of this development we realized that while the frequency domain has advantages for discriminating between ground clutter and meteorological signal, the autocorrelation domain is very powerful for estimating the spectral moments of the meteorological signal. Hence the processor is designed to perform certain tasks in the frequency domain, and then invert the Doppler spectrum to obtain the autocorrelation function. The autocorrelations for the first few lags are then stored and used subsequently in moment estimation algorithms. In this manner, the processor can take maximum advantage of both domains.

This development required considerable work in examining the theory of spectral moment estimation. Here we present some results of these explorations. The major finding is that the autocorrelation function is a very powerful way of representing the spectral moment information and hence provides an excellent technique for data compression. While this finding is not really new, the theory upon which it rests has not been appreciated in the past. The theoretical treatment is based on an asymptotic expansion of the radar autocorrelation function in terms of the central moments of the Doppler spectrum of velocities. The expansion leads to a new interpretation of the autocorrelation function and provides a general technique for creating a multiplicity of time-domain moment estimators for any moment of the Doppler spectrum. Moreover, the derivation of new estimators is reduced to a "back of the envelope" calculation by this simple approach. To illustrate the practical significance of the central moment expansion, we present a number of new estimators for various spectral moments, and compare the performances of three new spectral width estimators to that of the pulse-pair spectral width estimator. This evaluation is used to help illustrate the various trade-offs involved in the search for optimal estimators.

As a prelude, we present an interesting geometric

[1] Current affiliation SIGMET, Inc., Acton, MA 01720.

relationship between the autocorrelation function and the spectrum of Doppler velocities. This geometric relationship provides an intuitive approach to the inverse Fourier transform which permits one to deduce the properties of an autocorrelation function from the visual form of the Doppler spectrum.

2. Preliminary theoretical considerations

The reader is referred to a text on Fourier analysis or digital signal processing (e.g., Oppenheim and Schafer, 1975). The autocorrelation $R(\tau)$ and the power spectrum $S(\omega)$ for continuous signals are a Fourier transform pair, i.e.,

$$S(\omega) = \int_{-\infty}^{+\infty} R(\tau) e^{-j\omega\tau} d\tau, \tag{1}$$

$$R(\tau) = \frac{1}{2\pi} \int_{-\infty}^{\infty} S(\omega) e^{j\omega t} d\omega. \tag{2}$$

The autocorrelation of a continuous signal $A(t)$ is

$$R(\tau) = \lim_{T\to\infty} \frac{1}{T} \int_{-T/2}^{+T/2} A^*(t) A(t+\tau) dt, \tag{3}$$

where the asterisk denotes complex conjugation.

These formulae are convenient for analytical work, but a pulsed Doppler radar samples each range bin at discrete intervals τ_S for a finite time $N\tau_S$ (N radar pulses). The discrete Fourier transform (DFT) of an N-point periodic sequence A_n (i.e., $A_n = A_{n+N}$) is given by

$$F_k = \sum_{n=0}^{N-1} A_n e^{-j2\pi kn/N}, \tag{4}$$

with inverse transform

$$A_n = \frac{1}{N} \sum_{k=0}^{N-1} F_k e^{j2\pi kn/N}. \tag{5}$$

An estimator for the power spectrum is

$$S_k = \frac{1}{N} F_k F_k^*. \tag{6}$$

The discrete inverse transform of S_k is the circular autocorrelation of the periodic sequence A_n, i.e.,

$$\mathcal{R}(n\tau_s) = \frac{1}{N} \sum_{k=0}^{N-1} A_k^* A_{k+n}, \tag{7}$$

in which one uses the assumption of periodicity. Radar signals are not periodic, and one usually performs time domain estimates of the autocorrelation via,

$$R(n\tau_s) = \frac{1}{N - |n|} \sum_{k=0}^{N-|n|-1} A_k^* A_{k+n}. \tag{8}$$

Thus for a given N-point sequence,

$$\mathcal{R}(n\tau_s) \neq R(n\tau_s) \tag{9}$$

except for $n = 0$. However, for N large compared to n,

$$\mathcal{R}(n\tau_s) \sim R(n\tau_s) \tag{10}$$

to a high degree of accuracy.

3. A geometric interpretation for $R(\tau)$

Consider a discrete, N-point Doppler power spectrum estimate S_k where we let

$$k = -\frac{N}{2}, -\frac{N}{2} + 1, \ldots, 0, \ldots, \frac{N}{2} - 1. \tag{11}$$

For convenience, N is assumed to be even. The corresponding frequency shifts are

$$\omega_k = \frac{2\omega_u k}{N} = \frac{2\pi k}{N\tau_s}, \tag{12}$$

where ω_u is the unambiguous frequency shift, τ_s the time between radar pulses and

$$\tau_s \omega_u = \pi. \tag{13}$$

An example of a 16-point power spectrum is shown in Fig. 1a.

Suppose that we wanted to estimate the mean of this power spectrum in the frequency domain. One way is to define vectors $\mathbf{q}_k$ in the complex plane having amplitude S_k and phase $\pi\omega_k/\omega_u$, i.e.,

$$q_k = S_k e^{j\pi\omega_k/\omega_u} = S_k e^{j2\pi k/N}. \tag{14}$$

Fig. 1b shows a plot of the vectors $\mathbf{q}_k$ in the complex plane for the spectrum in Fig. 1a. The sum of the vectors $\mathbf{q}_k$ is also shown in Fig. 1b. For a symmetric power spectrum, the sum of $\mathbf{q}_k$ will point in the direction of the mean frequency shift. Note that white noise cancels itself in the vector sum and thus, on ensemble average over many realizations, makes no contribution. Also, for narrow spectra, the length of the resultant vector will be approximately equal to the signal power. A broader Doppler spectrum will have a greater number of vectors $\mathbf{q}_k$ pointing away from the net vector, hence the magnitude of the sum is less for broader spectra that have the same signal power.

Analytically, the vector sum is

$$\sum_{k=-N/2}^{(N/2)-1} \mathbf{q}_k = \sum_{k=-N/2}^{(N/2)-1} S_k e^{j2\pi k/N}, \tag{15}$$

which is N times the discrete inverse transform of S_k for $n = 1$ and is an estimator for $R(\tau_s)$—the autocorrelation for lag τ_s. Hence the pulse-pair mean frequency estimator

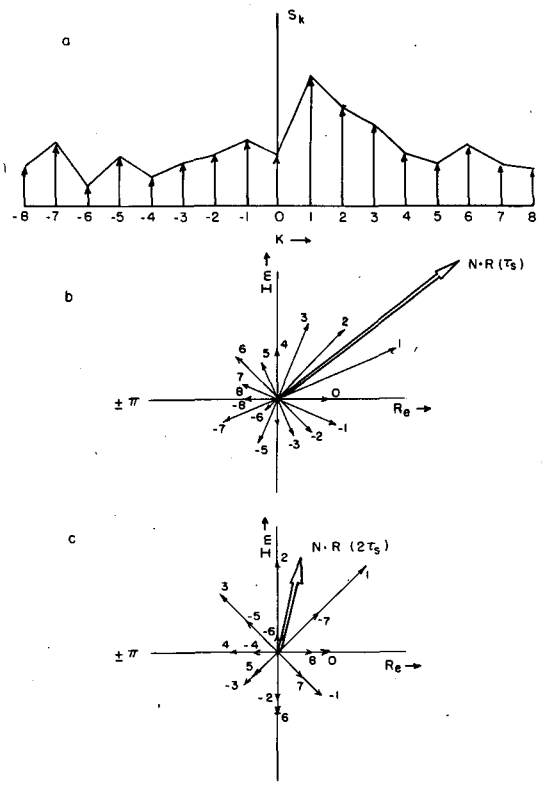

FIG. 1. (a) A 16-point discrete Doppler spectrum with the DC at $k = 0$. (b) Polar representation of the spectrum in the complex plane. The positive real axis corresponds to DC. (c) As in (b) except that the angle of each component is doubled. In both parts (b) and (c), the bold vector is the sum of the individual components.

$$\hat{\bar{\omega}} = \frac{1}{\tau_s} \arg[\hat{R}(\tau_s)], \tag{16}$$

where the caret denotes an estimator, can be interpreted as the argument of the sum of the vectors $\mathbf{q}_k$. This geometric interpretation illustrates several well-known properties of the pulse-pair mean estimator such that it is unbiased by white noise and unbiased for symmetric Doppler spectra. It can also be used to illustrate that the pulse pair mean is only slightly biased for highly skewed spectra. It also provides a qualitative demonstration of the relationship between the magnitude of $R(\tau_s)$ and the variance of the Doppler spectrum, i.e., for broader spectra, $|R(\tau_s)|$ is reduced. Similarly, one can show that the autocorrelation for the nth lag $R(n\tau_s)$ can be interpreted as the sum of vectors having magnitude S_k and phase $n\Pi\omega_k/\omega_u$. For example, $N \cdot R(2\tau_s)$ can be determined geometrically by summing

$$N \cdot R(2\tau_s) = \sum_{k=-N/2}^{(N/2)-1} S_k e^{2j(2\pi k/N)}. \tag{17}$$

This is shown in Fig. 1c for the spectrum in Fig. 1a. Since the angle of each component is doubled, the vectors are more divergent from the direction of the sum and hence contribute less of their total length to $|R(2\tau_s)|$ than for $|R(\tau_s)|$. Thus $|R(2\tau_s)|$ must be less than $|R(\tau_s)|$ which is well-known. Fig. 1c also serves to illustrate another well-known property of symmetric spectra,

$$\arg[R(2\tau_s)] = 2 \arg[R(\tau_s)]. \tag{18}$$

We have found this geometric interpretation to be a very useful conceptual tool in qualitative discussions of Doppler spectra and their corresponding autocorrelation functions. For example, suppose that one adds a high-pass filter to remove ground clutter (low frequency) bias from pulse-pair velocity estimates. What happens to the pulse-pair estimates when only white noise is present in the signal? Fig. 2a shows a hypothetical spectrum of white noise for this situation and Fig. 2b shows the corresponding vector representation. The sum will clearly point toward $\pm\pi$. Thus the ground clutter filter introduces a bias toward $\pm\omega_u$ which is largest when the ground clutter and meteorological power are weak as compared to the noise power.

4. A central moment expansion for the autocorrelation function

Moment expansions of functions are fairly common in probability theory and indeed the relationship between spectral moments and derivatives of the autocorrelation function is used in the classical derivation of the pulse-pair estimators for mean and variance (e.g., Miller and Rochwarger, 1972). The *central* moment expansion presented here has the important property that its convergence is not affected by the position of the spectrum in the frequency domain. This is not the case for an expansion in terms of the

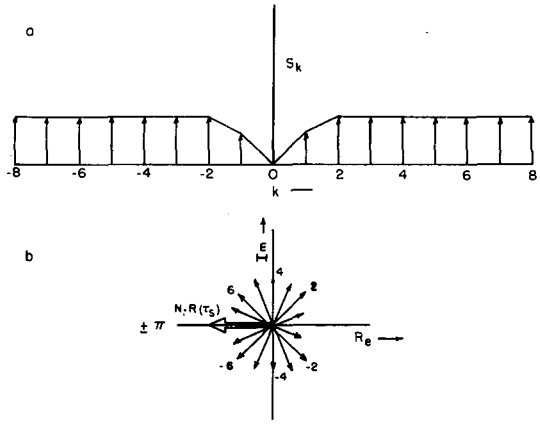

FIG. 2. (a) A 16-point discrete Doppler spectrum of white noise and a notch filter applied near DC. (b) The polar representation of the spectrum in (a) and the vector sum of the components.

moments of the Doppler spectrum since these are dependent on both the spectral shape and spectral mean, while central moments depend only on spectral shape.

We derive the central moment expansion by performing McLauren series expansions for the argument and magnitude of $R(\tau)$ and observing that each term is a central moment of the Doppler spectrum $S(\omega)$. We will neglect white noise for now and consider a continuous power spectrum $S(\omega)$. The autocorrelation can be written as

$$R(\tau) = \frac{h(\tau)}{2\pi} e^{jg(\tau)}, \tag{19}$$

where

$$h(\tau) = [A^2 + B^2]^{1/2}, \tag{20}$$

$$g(\tau) = \arctan\left[\frac{B}{A}\right], \tag{21}$$

and

$$A \equiv \text{Re}[2\pi R(\tau)] = \int_{-\infty}^{+\infty} S(\omega) \cos\omega\tau d\omega, \tag{22}$$

$$B \equiv \text{Im}[2\pi R(\tau)] = \int_{-\infty}^{+\infty} S(\omega) \sin\omega\tau d\omega. \tag{23}$$

We shall refer to h as simply the magnitude and g the argument of $R(\tau)$. Using (20)–(23) one can show that h is an even function of τ while g is odd.

The formal expansions for h and g are

$$h(\tau) = \frac{h_0}{0!} + \frac{h_0'\tau}{1!} + \frac{h_0''\tau^2}{2!} + \cdots, \tag{24}$$

$$g(\tau) = \frac{g_0}{0!} + \frac{g_0'\tau}{1!} + \frac{g_0''\tau^2}{2!} + \cdots, \tag{25}$$

where the subscript zero indicates evaluation at $\tau = 0$. Because h is even, we expect that all odd derivatives will be identically zero leaving only terms having even powers of τ. Similarly all even powers of τ should vanish from the expansion for g.

The derivatives of h and g can be determined from (20) and (21) in terms of the derivatives of A and B which can be determined from (22) and (23). The details are given in the Appendix. The result of this tedious process is

$$\left.\begin{aligned} h_0 &= S_0 \\ h_0' &= 0 \\ h_0'' &= -S_0\mathcal{M}_2 \\ h_0''' &= 0 \\ h_0^{iv} &= S_0\mathcal{M}_4 \\ h_0^{v} &= 0 \\ h_0^{vi} &= -S_0(\mathcal{M}_6 - 10\mathcal{M}_3^2) \end{aligned}\right\} \tag{26}$$

and

$$\left.\begin{aligned} g_0 &= 0 \\ g_0' &= \bar{\omega} \\ g_0'' &= 0 \\ g_0''' &= -\mathcal{M}_3 \\ g_0^{iv} &= 0 \\ g_0^{v} &= \mathcal{M}_5 - 10\mathcal{M}_2\mathcal{M}_3 \end{aligned}\right\}, \tag{27}$$

where the signal power is

$$S_0 = \int_{-\infty}^{+\infty} S(\omega)d\omega; \tag{28}$$

the nth central moment is

$$\mathcal{M}_n = \frac{1}{S_0}\int_{-\infty}^{+\infty} (\omega - \bar{\omega})^n S(\omega)d\omega, \tag{29}$$

and the mean of the Doppler spectrum is,

$$\bar{\omega} = \frac{1}{S_0}\int_{-\infty}^{+\infty} \omega S(\omega)d\omega. \tag{30}$$

Note that $\mathcal{M}_0 = 1$, $\mathcal{M}_1 = 0$, $\mathcal{M}_2$ is the variance and $\mathcal{M}_3$ we shall call the skewness. All odd central moments $\mathcal{M}_{2n+1}$ $(n = 1, 2, \cdots)$ are identically zero if the Doppler spectrum is symmetric.

Substituting expressions for the h_0 and g_0 derivatives into the expansions (24) and (25) for h and g, we obtain

$$h(\tau) = S_0\left[1 - \frac{\mathcal{M}_2\tau^2}{2!} + \frac{\mathcal{M}_4\tau^4}{4!} - \frac{(\mathcal{M}_6 - 10\mathcal{M}_3^2)}{6!} + \cdots\right], \tag{31}$$

$$g(\tau) = \bar{\omega}\tau - \frac{\mathcal{M}_3\tau^3}{3!} + \frac{(\mathcal{M}_5 - 10\mathcal{M}_2\mathcal{M}_3)\tau^5}{5!} - \cdots. \tag{32}$$

The next higher order terms have not been deduced but for a symmetric spectrum, one can show that in general,

$$h(\tau) = S_0 \sum_{n=0}^{\infty} (-1)^n \frac{\overline{\omega^{2n}}\tau^{2n}}{(2n)!}, \tag{33}$$

$$g(\tau) = \bar{\omega}\tau, \tag{34}$$

(see Appendix). As with any Taylor series expansion, convergence is more rapid when τ and/or the derivatives of h and g (the central moments) are small. Hence the series for h and g converge more rapidly for small lag times and narrow, near symmetric spectra.

These expansions for h and g illustrate several important properties of the autocorrelation function.

First, h depends primarily on the even central moments. It is not until the fourth term in (31) that there is any dependence on spectral asymmetry. Similarly, the first two terms in the $g(\tau)$ expansion (32) do not depend on the even central moments. Passarelli and Siggia (1981) had inferred a complete decoupling of the even and odd central moments, but the explicit calculation presented here shows that this is only approximately true. One can use the expansions (to the order they are known) to show that $g(\tau)$ is not changed when an arbitrary Doppler spectrum is convolved with a zero-mean symmetric function. To the extent that this is a good model of the effect of turbulence on vertical incidence Doppler spectra of rain, Dazhang and Passarelli (1983) use this invariance of g to deduce drop size spectra.

Another property that is illustrated by the expansion for g is how asymmetry will affect the pulse-pair mean frequency estimator $\hat{\bar{\omega}}_{pp}$, i.e.,

$$\hat{\bar{\omega}}_{pp} = \frac{1}{\tau_s} g(\tau_s), \tag{35}$$

where τ_s is the time between radar pulses. While this is exactly true for symmetric spectra, it is not true for asymmetric spectra. The expansion for g provides an explicit look at the first-order effect of asymmetry on the pulse-pair estimator. This will be discussed in the next section.

Since a pulsed Doppler radar is constrained to sample the time series at discrete intervals, spaced τ_s apart, it is convenient to define a nondimensional frequency shift on $[-\pi, \pi]$, i.e., let

$$\theta = \frac{\omega}{\omega_u} \cdot \pi = \omega \tau_s. \tag{36}$$

The Doppler power spectrum can be transformed to this new space via

$$s(\theta) = S(\omega)\left|\frac{d\omega}{d\theta}\right| = \frac{1}{\tau_s} S(\omega). \tag{37}$$

The central moments of $S(\theta)$ are

$$M_n = \frac{1}{S_0}\int_{-\pi}^{+\pi} S(\theta - \theta)^{-n} d\theta = \mathcal{M}_n {\tau_s}^n \tag{38}$$

where $\bar{\theta}$ is the mean of $S(\theta)$,

$$\bar{\theta} = \bar{\omega}\tau_s. \tag{39}$$

For $\tau = k\tau_s$, where k is an integer, the expansions become

$$h(k\tau_s) \equiv h_k = S_0\left\{1 - \frac{M_2 k^2}{2!} + \frac{M_4 k^4}{4!} - \cdots\right\} \tag{40}$$

and

$$g(k\tau_s) \equiv g_k = k\bar{\theta} - \frac{M_3 k^3}{3!} + \cdots. \tag{41}$$

The presence of white noise will only bias $h(k\tau_s)$ when $k = 0$ and will not bias $g(k\tau_s)$. To account for white noise, an additional term must be added to the expansion for h, i.e.,

$$h(k\tau_s) = N_0\delta(k\tau_s) + \cdots \tag{42}$$

where N_0 is the noise power and δ is the Dirac delta function.

The practical value of these expansions is their use in time-domain moment estimation. The pulse-pair mean and variance estimators are a subset of an entire class of spectral estimators which can be derived from the expansions. This topic is explored in the next section.

5. Use of the expansions in the derivation of time-domain moment estimators

a. General technique

The expansions for $h(\tau)$ and $g(\tau)$ provide a formal approach for generating time domain algorithms for determining any moment of the Doppler spectrum. The general approach is to truncate the expansions (40) and (41) for h and g, and then use measurements of $R(\tau)$ at a sufficient number of lags so as to obtain a closed system of equations. In implementing this procedure, one finds it useful to measure the average noise power $\hat{N}_0$. Also, $g(k\tau_s)$ must be unfolded relative to $g(\tau_s)$. For near symmetric spectra, the relation

$$\hat{g}(k\tau_s) \sim k\hat{g}(\tau_s), \tag{43}$$

where the caret indicates that these are estimates, is usually adequate for unfolding the higher order lags.

In the following sections, we present examples of this procedure. The notation $\hat{h}_k$ shall denote an estimate of $h(k\tau_s)$, $\hat{M}_k$ an estimator for the kth central moment and $\hat{N}_0$ an estimator for the noise power.

b. The [0, 1] algorithms (the pulse-pair)

The time domain moment estimators based on measurements of $R(0)$ and $R(\tau_s)$ shall be called the [0, 1] algorithms. Given $\hat{h}_0$, $\hat{h}_1$, $\hat{g}_1$ and an estimate of $\hat{N}_0$ we can form the following two systems of equations by retaining two terms in the expansion for h and one term in the expansion for g, i.e.,

$$\left.\begin{aligned} \hat{h}_0 &= \hat{S}_0 + \hat{N}_0 \\ \hat{h}_1 &= \hat{S}_0\left(1 - \frac{\hat{M}_2}{2!}\right) \end{aligned}\right\}, \tag{44}$$

$$\hat{g}_1 = \hat{\bar{\theta}}. \tag{45}$$

The equation for $\hat{\bar{\theta}}$ is the familiar pulse-pair mean estimator. Solving the system (44), we obtain

$$\hat{S}_0 = \hat{h}_0 - \hat{N}_0, \tag{46}$$

assuming that $\hat{N}_0 = \bar{N}_0$, and

$$\hat{M}_2 = 2\left[1 - \frac{\hat{h}_1}{\hat{S}_0}\right], \tag{47}$$

which is the familiar pulse-pair variance estimator. Note that a signal-to-noise ratio correction is implicit in the expression for $\hat{S}_0$.

The expansions provide a new interpretation for the pulse-pair mean estimator in that it is the lowest order mean estimator regardless of the form of the Doppler spectrum. The next higher order estimator for the mean, using lags [0, 1, 2], includes a correction for skewness and is given below.

c. *The [0, 1, 2] algorithms*

Given N_0, h_0, h_1, h_2, g_1 and g_2, one can form the following two systems of linear equations

$$\left.\begin{aligned} \hat{h}_0 &= \hat{S}_0 + \hat{N}_0 \\ \hat{h}_1 &= \hat{S}_0\left(1 - \frac{\hat{M}_2}{2!} + \frac{\hat{M}_4}{4!}\right) \\ \hat{h}_2 &= \hat{S}_0\left[1 - \frac{\hat{M}_2}{2!}(2)^2 + \frac{\hat{M}_4}{4!}(2)^4\right] \end{aligned}\right\}, \tag{48}$$

$$\left.\begin{aligned} \hat{g}_1 &= \hat{\bar{\theta}} - \frac{\hat{M}_3}{3!} \\ \hat{g}_2 &= 2\hat{\bar{\theta}} - \frac{\hat{M}_3}{3!}(2)^3 \end{aligned}\right\}. \tag{49}$$

Solving for the moments, we get

$$\left.\begin{aligned} \hat{S}_0 &= \hat{h}_0 - \bar{N}_0 \\ \hat{M}_2 &= \frac{5}{2} - \frac{1}{\hat{S}_0}\left(\frac{8\hat{h}_1}{3} - \frac{\hat{h}_2}{6}\right) \\ \hat{M}_4 &= 6 - \frac{1}{\hat{S}_0}(8\hat{h}_1 - 2\hat{h}_2) \\ \hat{\bar{\theta}} &= \frac{4\hat{g}_1}{3} - \frac{\hat{g}_2}{6} \\ \hat{M}_3 &= 2\hat{g}_1 - \hat{g}_2 \end{aligned}\right\}. \tag{50}$$

The [0, 1, 2] mean estimator includes a correction for skewness. Note that for a symmetric spectrum $2g_1 = g_2$ so that $\bar{\theta} = g_1$ and $M_3 = 0$. Also note that for $S(\theta) = S_0\delta(\theta - \bar{\theta})$ then $S_0 = h_1 = h_2$ so that $M_2 = M_4 = 0$, as one would expect. Aside from providing estimates of higher order moments, the greater number of terms employed in the truncated expansions can improve the accuracy of the estimators for the lower order moments.

Note that if one assumes that the spectrum is perfectly symmetric then each measurement g_n yields a mean estimator, i.e.,

$$\left.\begin{aligned} \hat{g}_1 &= \hat{\bar{\theta}}_1 \\ \hat{g}_2 &= 2\hat{\bar{\theta}}_2 \\ &\vdots \quad \vdots \\ \hat{g}_n &= n\hat{\bar{\theta}}_n \end{aligned}\right\}. \tag{51}$$

This approach has been dubbed the "poly-pulse-pair" approach by Lee (see Strauch *et al.*, 1978) who proposes that for weak, narrow, symmetric spectra, the average of these velocity estimates can be a better estimator than the standard pulse-pair (i.e., $\hat{g}_1 = \hat{\bar{\theta}}$). Simulations employing symmetric spectra are used to demonstrate this, but it must be recognized that for skewed spectra the estimator will be biased and that in nature, sampling statistics and gradients of velocity and reflectivity produce skewed spectra.

d. *Optimal estimation*

The accuracy of these estimators is governed by two factors—the rate of convergence of the series (estimator bias) and the accuracy of the estimates of h and g. For broad (or highly skewed) spectra one requires more terms in the expansion for h (or g) since the higher order moments have greater influence on h (or g). For narrow (or near symmetric) spectra, the higher order moments are small and only a few terms are required in the expansion for h (or g). Hence one would anticipate that moment estimation would be improved for broad (or highly skewed) spectra by the incorporation of additional lags. However, for narrow (near symmetric) spectra the incorporation of additional lags may actually degrade the estimator since the additional lag provides little information and carries with it the errors inherent in the estimation of the autocorrelation function. This trade-off between the variance introduced by incorporating the estimates of the higher order lags and the variance due to the estimator bias (the accuracy of the expansions) implies that for a given moment of a given spectrum, there is one estimator that is optimal.

Zrnic' (1979) points out the radar meteorological implications of optimal estimation. The goal is to provide accurate spectral moment estimation with as few pulses as possible. He states that for optimum processing one needs estimates of the autocorrelation function at all available lags. The expansions demonstrate that it is the low order lags of the autocorrelation function which contain most of the low-order moment information. Hence while in principal an optimal moment estimator may require complete knowledge of the autocorrelation function, in practice only a few lags may be required to obtain the optimal estimator for the low order moments. The expansions provide a family of possible estimators for this selec-

tion process, as well as an intuitive understanding of the trade-offs. A full exploration of how the expansions can be used in deriving optimal estimators is beyond the scope of this paper. However, in the next section we present an evaluation of three new spectral width estimators which illustrates the problem.

6. Evaluation of three new spectral width estimators

In this section, Doppler spectral width estimators based on [0, 1] (the pulse-pair), [0, 1, 2], [1, 2] and [1, 2, 3] algorithms are evaluated for simulated Gaussian Doppler spectra. We shall use the term *spectral variance* or *variance* to refer to the second central moment of the Doppler spectrum of weather (i.e., M_2 for the nondimensional spectrum on $[-\pi, \pi]$). Strictly, the spectral width is the square root of the variance—the standard deviation. Derivations for the [0, 1] and [0, 1, 2] variance estimators have been presented. The [1, 2] and [1, 2, 3] variance estimators can be derived in an analogous manner yielding (dropping the ^ notation),

$$M_2[1, 2] = 2\left(\frac{h_1 - h_2}{4h_1 - h_2}\right), \tag{52}$$

$$M_2[1, 2, 3] = M_2[1, 2]\left[1 + \frac{M_4[1, 2, 3]}{4!}\frac{(16h_1 - h_2)}{(h_1 - h_2)}\right], \tag{53}$$

where the kurtosis M_4 based on [1, 2, 3] is

$$M_4[1, 2, 3] = 4!\,\frac{(h_1 - h_2)(9h_1 - h_3) - (h_1 - h_3)(4h_1 - h_2)}{(81h_1 - h_3)(4h_1 - h_2) - (16h_1 - h_2)(9h_1 - h_3)}. \tag{54}$$

The [1, 2, 3] variance estimator has been expressed in terms of the [1, 2] variance estimator to illustrate the correction obtained when the additional lag $R(3\tau_s)$ is included. Since the correction is proportional to $M_4[1, 2, 3]$, $M_2[1, 2]$ and $M_2[1, 2, 3]$ are approximately equal for narrow spectra. Note that neither $M_2[1, 2]$ nor $M_2[1, 2, 3]$ requires a noise estimate.

The bias of each estimator can be examined by considering a pure Gaussian spectrum whose autocorrelation at lag n is

$$R_n = \frac{S_0}{2\pi} e^{-\sigma^2 n^2/2} e^{jn\bar{\theta}}, \tag{55}$$

where σ^2 is the variance of the nondimensional spectrum on $[-\pi, \pi]$. The variance estimates as functions of spectral width σ are shown in Fig. 3 along with the actual variance σ^2. All four estimators do an excellent job for narrow widths, but at large widths they depart significantly from the actual variance. To emphasize the relative error, Fig. 4 shows the absolute value of the percentage error in the estimators as a function of the spectral width. The order of performance of the estimators, from best to worst, is $M_2[0, 1, 2]$, $M_2[0, 1]$, $M_2[1, 2, 3]$ and $M_2[1, 2]$.

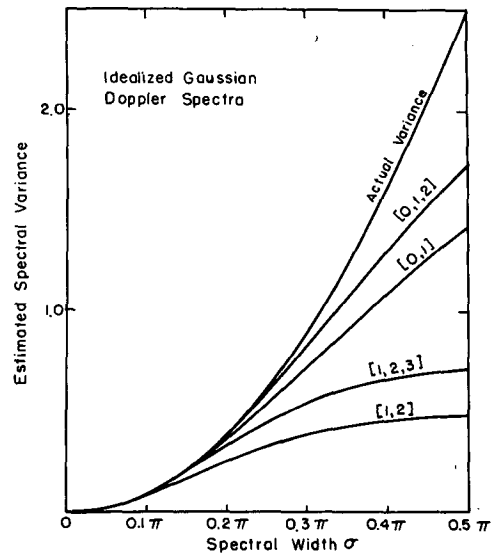

FIG. 3. Estimated spectral variance versus spectral width for the [1, 2], [1, 2, 3], [0, 1] (the pulse pair) and [0, 1, 2] algorithms for idealized Gaussian Doppler spectra. The spectral domain is $[-\pi, \pi]$.

The relative performances of the estimators can be understood by considering the convergence of the expansion for $h(\tau)$. The convergence is more rapid when n is small and the accuracy of the expansion is improved as more terms are added. Thus the [0, 1, 2] estimator is better than the [0, 1] estimator (the

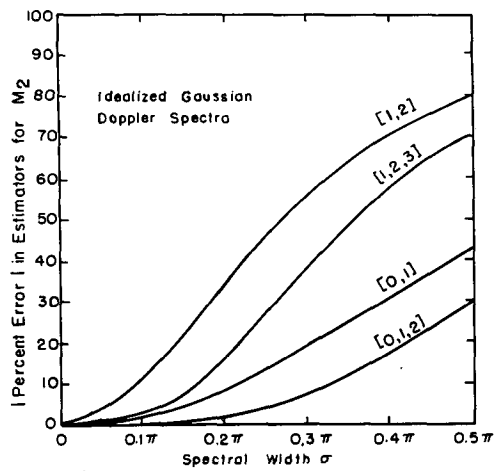

FIG. 4. The absolute value of the percentage error in the variance estimators versus spectral width for idealized Gaussian spectra, Estimators are indicated on the curves.

pulse-pair) because of the extra term. The [0, 1] estimator is better than the [1, 2] estimator because it employs lower order lags (smaller n). Based on this analysis one would choose the [0, 1, 2] variance estimator. However, one must recall that for this case, there is no noise and the autocorrelations are known precisely.

Figs. 5 and 6 show results from simulated 128-point autocorrelations containing white noise and the statistical properties of Gaussian weather echoes for signal-to-noise ratios (SNR) of 10 and 0 dB, respectively, (e.g., Sirmans and Bumgarner, 1975). To emphasize the relative error, the average absolute value of the percentage deviation of the estimated variance, from the true variance is plotted as a function of the spectral width σ. Forty realizations were used for each spectral width.

As suggested by the discussion in Section 5, each variance estimator has an optimal region where the estimator error is a minimum. For broad spectra, the results reflect the biases shown for the pure Gaussian spectra—the [0, 1, 2] is the best estimator followed by the [0, 1], [1, 2, 3] and [1, 2] estimators. However, for narrow spectra, this order of performance is completely reversed. While the errors in the estimators are somewhat larger at 0 dB SNR (Fig. 6) than at 10 dB SNR (Fig. 5) the ordering of the performances is not changed.

The order of performance for small spectral widths can be understood by considering the number of fundamental estimates incorporated into the algorithms (e.g., $\bar{N}_0$, h_0, h_1, $h_2 \cdots$). Each of these carries with it the penalty of additional estimator variance. For example, the [0, 1] variance estimator employs the set of estimates $\{\bar{N}_0, h_0, h_1\}$ while the [0, 1, 2] estimator employs $\{\bar{N}_0, h_0, h_1, h_2\}$. The additional lag h_2 carries little additional information for narrow spectra; hence the errors inherent in estimating h_2 apparently degrade the estimator. Similarly the [1, 2] estimator employs $\{h_1, h_2\}$ while the [1, 2, 3] estimator employs $\{h_1, h_2, h_3\}$. Of all the estimators, the [1, 2] uses the fewest fundamental estimates and performs best for narrow spectral widths. This implies that the incorporation of h_3 into the estimator carries with it more estimator variance than it does new information.

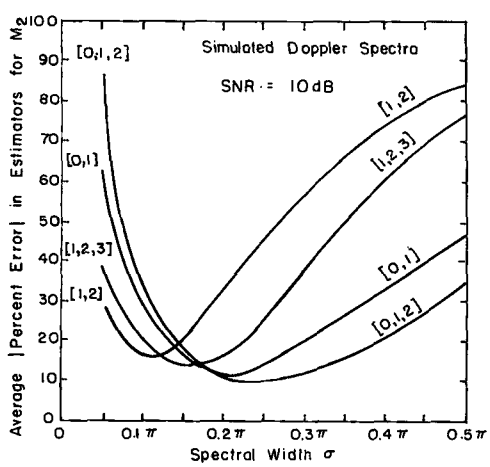

FIG. 5. Average absolute value of the percentage error in the variance estimators versus spectral width for simulated Gaussian weather signals and white noise. The average signal-to-noise ratio is 10 dB.

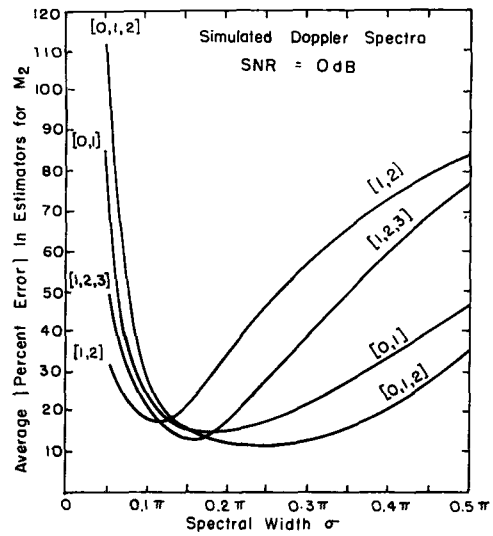

FIG. 6. As in Fig. 5 except for a signal-to-noise ratio of 0 dB.

As implied in Section 5, the optimal estimator is the one that employs the minimum number of fundamental estimates so as to minimize statistical fluctuations, and still retains a sufficient number of terms in the expansions to minimize estimator bias. In seeking the optimal estimator the question is, Which lags are the most effective? Clearly, for broad spectra, one requires contiguous, low order lags to assure optimal convergence of the expansions (minimize estimator bias). For very narrow spectra, convergence is not a problem, and one wants to use only two fundamental estimates (the minimum number) to estimate spectral width. Now the question is, Which two lags are optimal for narrow spectra? This issue introduces a slightly different class of width estimators for narrow spectra which is discussed here.

For very narrow spectra, the performance of a variance estimator would be improved if one could increase the spectral width in the domain $[-\Pi, \Pi]$. One way of doing this is to reduce the pulse repetition frequency (increase τ_s) and sample over a longer dwell time so that one maintains the same number of pulses. An equivalent way of doing this without increasing the dwell time is to formulate a variance estimator by using alternating lags. For example, sup-

pose that h_0, N_0 and h_2 are measured, then the corresponding expansions become

$$\left.\begin{aligned} h_0 &= S_0 + \bar{N}_0 \\ h_2 &= S_0(1 - 2\sigma^2) \end{aligned}\right\}. \tag{56}$$

The corresponding variance estimator is

$$\sigma^2 = \frac{1}{2}\left(1 - \frac{h_2}{S_0}\right). \tag{57}$$

This variance estimator is identical to the standard pulse pair [0, 1] estimator evaluated at half the pulse repetition frequency but double the dwell time (same total number of pulses). Of course the [0, 2] estimator has the advantage that the estimates of h_0 and h_2 are made in half the time with the same number of pulses. The relative performance of the [0, 2] estimator can be determined from the [0, 1] estimator curve by halving the spectral width values on the abscissa of Figs. 5 and 6 which illustrates that the [0, 2] algorithm is superior to the [0, 1] algorithm for narrow spectra.

Intuitively, it is the differences between the h_k estimates that contain the spectral width information, and when the spectral width is narrow, these differences are small, i.e., a small difference between h_k and h_{k+1} corresponds to a relatively large difference in the variance estimate. This means that the h_k must be estimated to great accuracy. For narrow spectra the statistical fluctuations in the h_k estimates can dominate the differences. The differences between the h_{2k} are larger and hence contain more information on the spectral width. Provided that the statistical errors in the measurement of the h_{2k} are approximately the same as for the h_k (true for narrow spectra), then the estimate of spectral width using say [0, 2, 4] should be superior to [0, 1, 2] for spectral widths less than some value.

Returning to Figs. 5 and 6, we observe that for narrow spectra, the [1, 2, 3] estimator is far superior to the [0, 1] estimator even though they both employ three fundamental estimates. The inclusion of the higher order lag h_3 provides additional information on the variance that the [0, 1] estimator does not have, i.e., the differences $(h_1 - h_3)$ and $(h_2 - h_3)$. If one were to drop h_2 to form the [1, 3] estimator, the performance would be superior to the [1, 2, 3] estimator because the errors due to h_2 would be eliminated, and most of the variance information is contained in the $h_1 - h_3$ difference. A [1, 3] estimator would be superior to the [1, 2] estimator since both employ two fundamental estimates, but there is more variance information in the $h_1 - h_3$ difference than in the $h_1 - h_2$ difference.

In general, the implementation of a single width estimator does not appear to be a very good idea. However, this is what is currently done on most meteorological Doppler radars. Of course the particular radar application has a strong bearing on the estimation procedure. For example, the accurate measurement of narrow spectral widths may not be an issue in some applications, in which case one may choose an estimator that minimizes bias, e.g., the [0, 1, 2]. While this approach is easy to implement, the sacrifice of the narrow spectral width information is unnecessary and could even lead to an unacceptable number of false warnings of broad spectra. For real-time spectral width estimation, it is better to calculate a limited number of estimates, determine the probable range of spectral width and select the estimator that is optimal for that range. This procedure can be based upon modeling studies of the type presented here.

7. Summary and conclusions

The geometric and asymptotic interpretations provide some rather simple intuitive tools for understanding apparently complex relationships between the autocorrelation function and the Doppler spectrum of velocities. The central moment expansion of the autocorrelation function offers a unified theoretical framework for deriving time-domain moment estimates and illustrates the trade-offs in optimal moment estimation.

The emphasis here has been to illustrate how one goes about assessing a problem in moment estimation rather than proposing specific solutions to specific problems. However, it is clear that the current practice of recording only the pulse-pair parameters (e.g., $\bar{N}_0$, h_0, h_1, g_1) is not optimal. The addition of h_2 and g_2 opens up the possibility of three additional spectral width estimators ([0, 1, 2], [0, 2], [1, 2], [0, 1] as opposed to just [0, 1]); two additional velocity estimators ([1], [2], [1, 2] as opposed to just [1]); a skewness estimator (based on [1, 2]) and a kurtosis estimator (based on [0, 1, 2]). This list does not include the possible parametric estimators (e.g., Srivastava *et al.*, 1979; Passarelli, 1983) for which one assumes a given form for the Doppler spectrum, such as Gaussian. Hence the addition of just one lag to the standard pulse-pair parameters provides a very large increase in flexibility.

Acknowledgments. The authors thank L. Manzi, J. Fulton and I. Kole for manuscript preparation. This work was sponsored by the National Science Foundation under Grants ATM-8013711 and ATM-8209375.

APPENDIX

Derivation of the Central Moment Expansions

Consider a Doppler spectrum $S(\omega)$ on $[-\infty, +\infty]$ having mean $\bar{\omega}$. Its autocorrelation is found by taking the inverse Fourier transform of $S(\omega)$, i.e.,

$$R(\tau) = \mathcal{F}^{-1}[S(\omega)] \equiv \frac{1}{2\Pi}\int_{-\infty}^{+\infty} S(\omega)e^{j\omega\tau}d\omega. \quad \text{(A1)}$$

Likewise,

$$S(\omega) = \mathcal{F}[R(\tau)] = \int_{-\infty}^{+\infty} R(\tau)e^{-j\omega\tau}d\tau. \quad \text{(A2)}$$

For convenience, the spectrum can be shifted to have zero mean by letting

$$s(\omega - \bar{\omega}) = S(\omega), \quad \text{(A3)}$$

where the mean of s is zero. By the frequency shifting property of the Fourier transform,

$$r(\tau)e^{j\bar{\omega}\tau} = R(\tau), \quad \text{(A4)}$$

where

$$r(\tau) = \mathcal{F}[s(\omega)] \quad \text{(A5)}$$

is the autocorrelation of the zero mean spectrum s. Hereafter we shall assume that $S(\omega)$ has zero mean, recognizing that the $\bar{\omega} \neq 0$ case can be recovered via (A4).

The autocorrelation $R(\tau)$ can be expressed as

$$R(\tau) = \frac{h(\tau)}{2\pi}e^{jg(\tau)} = \frac{A}{2\pi} + \frac{jB}{2\pi}, \quad \text{(A6)}$$

where

$$A \equiv 2\pi\ \mathrm{Re}[R(\tau)] = \int_{-\infty}^{+\infty} S(\omega)\cos\omega\tau d\omega, \quad \text{(A7)}$$

$$B \equiv 2\pi\ \mathrm{Im}[R(\tau)] = \int_{-\infty}^{+\infty} S(\omega)\sin\omega\tau d\omega, \quad \text{(A8)}$$

and

$$h = (A^2 + B^2)^{1/2}, \quad \text{(A9)}$$

$$g = \arctan\left(\frac{B}{A}\right). \quad \text{(A10)}$$

Here A, B, h and g are real functions since $S(\omega)$ is real; h is even and positive, and g is odd. Note that for $\bar{\omega} = 0$ and $S(\omega)$ symmetric, B and hence g are identically zero. As an aside we note that if $S(\omega)$ does not have zero mean, then by (A4),

$$\arg[R(\tau)] = \arg[r(\tau)e^{j\bar{\omega}\tau}], \quad \text{(A11)}$$

where $r(\tau)$ corresponds to the shifted zero-mean spectrum. If the spectrum is symmetric, then $\arg[r(\tau)] = 0$ so that $\arg[R(\tau)] = \bar{\omega}\tau$ which is the basis for the pulse-pair algorithm.

The formal Taylor expansions for h and g about $\tau = 0$ are

$$h(\tau) = h_0 + h_0'\tau + \frac{h_0''\tau^2}{2!} + \cdots, \quad \text{(A12)}$$

$$g(\tau) = g_0 + g_0'\tau + \frac{g_0''\tau^2}{2!} + \cdots, \quad \text{(A13)}$$

where the zero subscript indicates evaluation at $\tau = 0$. We anticipate that since h is even, all odd derivatives of h vanish at $\tau = 0$. Likewise, all even derivatives of g should vanish at $\tau = 0$. The derivatives of h and g can be found in terms of A and B by differentiating (A9) and (A10). For the derivatives of h one obtains:

$$\left.\begin{aligned} h &= (A^2 + B^2)^{1/2} \\ h' &= \frac{G}{h} \\ h'' &= \frac{1}{h}(G' - h'^2) \\ h''' &= \frac{1}{h}(G'' - 3h'h'') \\ h^{iv} &= \frac{1}{h}(G''' - 4h'h''' - 3h''^2) \\ h^{v} &= \frac{1}{h}(G^{iv} - 5h'h^{iv} - 10h''h''') \\ h^{vi} &= \frac{1}{h}(G^{v} - 6h'h^{v} - 15h''h^{iv} - 10h'''^2) \end{aligned}\right\}, \quad \text{(A14)}$$

where

$$\left.\begin{aligned} G &= AA' + BB' \\ G' &= AA'' + A'^2 + BB'' + B'^2 \\ G'' &= AA''' + 3A'A'' + BB''' + 3B'B'' \\ G''' &= AA^{iv} + 4A'A''' + 3A''^2 + BB^{iv} \\ &\quad + 4B'B''' + 3B''^2 \\ G^{iv} &= AA^{v} + 5A'A^{iv} + 10A''A''' \\ &\quad + \cdots + 10B''B''' \\ G^{v} &= AA^{vi} + 6A'A^{v} + 15A''A^{iv} \\ &\quad + 10A'''^2 + \cdots + 10B'''^2 \end{aligned}\right\}. \quad \text{(A15)}$$

Note that the terms in B are identical in form to the terms in A. The derivatives of A and B evaluated at $\tau = 0$ are found from (A7) and (A8) yielding:

$$\left.\begin{aligned} A_0 &= S_0 & B_0 &= 0 \\ A_0' &= 0 & B_0' &= S_0\bar{\omega} = 0 \\ A_0'' &= -S_0\overline{\omega^2} & B_0'' &= 0 \\ A_0''' &= 0 & B_0''' &= -S_0\overline{\omega^3} \\ A_0^{iv} &= S_0\overline{\omega^4} & B_0^{iv} &= 0 \\ A_0^{v} &= 0 & B_0^{v} &= S_0\overline{\omega^5} \\ A_0^{vi} &= -S_0\overline{\omega^6} & B_0^{vi} &= 0 \end{aligned}\right\}, \quad \text{(A16)}$$

where the moments are

$$\overline{\omega^n} = \frac{1}{S_0}\int_{-\infty}^{+\infty} \omega^n S(\omega)d\omega, \tag{A17}$$

and the signal power is

$$S_0 = \int_{-\infty}^{+\infty} S(\omega)d\omega. \tag{A18}$$

In this case where $\bar{\omega} = 0$, the moments are identically equal to the central moments $\mathcal{M}_n$,

$$\mathcal{M}_n = \frac{1}{S_0}\int_{-\infty}^{+\infty} (\omega - \bar{\omega})^n S(\omega)d\omega. \tag{A19}$$

Substituting (A16) into (A15) we obtain,

$$\left.\begin{array}{ll} G_0 = 0 & G_0''' = S_0{}^2\overline{\omega^4} + 3S_0{}^2\overline{\omega^2}{}^2 \\ G_0' = -S_0{}^2\overline{\omega^2} & G_0^{iv} = 0 \\ G_0'' = 0 & G_0^{v} = -S_0{}^2\overline{\omega^6} + 15S_0{}^2\overline{\omega^2}\,\overline{\omega^4} \\ & \quad + 10S_0{}^2\overline{\omega^3}{}^2 \end{array}\right\}. \tag{A20}$$

Substituting these results into (A14), we obtain the required derivatives of h evaluated at $\tau = 0$:

$$\left.\begin{array}{l} h_0 = S_0 \\ h_0' = 0 \\ h_0'' = -S_0\overline{\omega^2} \\ h_0''' = 0 \\ h_0^{iv} = S_0\overline{\omega^4} \\ h_0^{v} = 0 \\ h_0^{vi} = -S_0\{\overline{\omega^6} - 10\overline{\omega^3}{}^2\} \end{array}\right\}. \tag{A21}$$

The next higher order terms have not been derived and no general pattern has been deduced.

For the expansion of $g(\tau)$, the derivatives are:

$$\left.\begin{array}{l} g = \arctan\left\{\dfrac{B}{A}\right\} \\ g' = \dfrac{H}{Q} \\ g'' = \dfrac{1}{Q}(H' - Q'g') \\ g''' = \dfrac{1}{Q}(H'' - 2Q'g'' - Q''g') \\ g^{iv} = \dfrac{1}{Q}(H''' - 3Q'g''' - 3Q''g'' - Q'''g') \\ g^{v} = \dfrac{1}{Q}(H^{iv} - 4Q'g^{iv} - 6Q''g''' \\ \qquad - 4Q'''g'' - Q^{iv}g') \end{array}\right\}, \tag{A22}$$

where

$$\left.\begin{array}{l} H = AB' - BA' \\ H' = AB'' - BA'' \\ H'' = AB''' + A'B'' - B'A'' - BA''' \\ H''' = AB^{iv} + 2A'B''' - 2A'''B' - BA^{iv} \\ H^{iv} = AB^{v} + 3A'B^{iv} + 2A''B''' \\ \qquad - 2A'''B'' - 3A^{iv}B' - BA^{v} \end{array}\right\} \tag{A23}$$

and

$$\left.\begin{array}{l} Q = A^2 + B^2 \\ Q' = 2AA' + 2BB' \\ Q'' = 2(A'^2 + AA'' + B'^2 + BB'') \\ Q''' = 2(AA''' + 3A'A'' + 3B'B'' + BB''') \\ Q^{iv} = 2(AA^{iv} + 4A'''A' + 3A''^2 + 3B''^2 \\ \qquad + 4B'B''' + BB^{iv}) \end{array}\right\} \tag{A24}$$

With use of (A16), the values of the H and Q derivatives at $\tau = 0$ can be found in terms of the moments yielding,

$$\left.\begin{array}{l} H_0 = 0 \\ H_0' = S_0{}^2\bar{\omega} = 0 \\ H_0'' = -S_0{}^2\overline{\omega^3} \\ H_0''' = 0 \\ H_0^{iv} = S_0{}^2\overline{\omega^5} + 2S_0{}^2\overline{\omega^2}\,\overline{\omega^3} \end{array}\right\} \tag{A25}$$

and

$$\left.\begin{array}{l} Q_0 = S_0{}^2 \\ Q_0' = 0 \\ Q_0'' = -2S_0{}^2\overline{\omega^2} \\ Q_0''' = 0 \\ Q_0^{iv} = 2S_0{}^2\overline{\omega^4} + 6S_0{}^2\overline{\omega^2}{}^2 \end{array}\right\}. \tag{A26}$$

Inserting the values from (A25) and (A26) into (A22) we get the derivatives of g at $\tau = 0$, i.e.,

$$\left.\begin{array}{l} g_0 = 0 \\ g_0' = \bar{\omega} = 0 \\ g_0'' = 0 \\ g_0''' = -\overline{\omega^3} \\ g_0^{iv} = 0 \\ g_0^{v} = \overline{\omega^5} - 10\overline{\omega^3}\,\overline{\omega^2} \end{array}\right\}. \tag{A27}$$

Inserting the results from (A21) and (A27) into the formal expansions (A2) and (A3), we obtain

$$h(\tau) = S_0\left\{1 - \frac{\overline{\omega^2}\tau^2}{2!} + \frac{\overline{\omega^4}\tau^4}{4!} - \frac{(\overline{\omega^6} - 10\overline{\omega^3}^2)}{6!}\tau^6 + \cdots\right\}, \quad \text{(A28)}$$

$$g(\tau) = \frac{-\overline{\omega^3}\tau^3}{3!} + \frac{(\overline{\omega^5} - 10\overline{\omega^3}\,\overline{\omega^2})\tau^5}{5!} - \cdots. \quad \text{(A29)}$$

For the more general case when $\bar{\omega} \neq 0$, one can use (A4) to show that

$$h(\tau) = N_0\delta(\tau) + S_0\left[1 - \frac{\mathcal{M}_2\tau^2}{2!} + \frac{\mathcal{M}_4\tau^4}{4!} - \frac{(\mathcal{M}_6 - 10\mathcal{M}_3^2)\tau^6}{6!} + \cdots\right] \quad \text{(A30)}$$

and

$$g(\tau) = \bar{\omega}\tau - \frac{\mathcal{M}_3\tau^3}{3!} + \frac{(\mathcal{M}_5 - 10\mathcal{M}_2\mathcal{M}_3)\tau^5}{5!} + \cdots, \quad \text{(A31)}$$

where we have added the term $N_0\delta(\tau)$ to account for the power contained in white noise as explained in the text.

For the special case of a symmetric spectrum centered about DC, $B(\tau)$ and hence $g(\tau)$ are identically zero. Hence $h(\tau) = A(\tau)$. The Taylor series expansion for $A(\tau)$ can be found from the derivatives $A(16)$ yielding,

$$h(\tau) = S_0 \sum_{n=0}^{\infty} \frac{(-1)^n \mathcal{M}_{2n}\tau^{2n}}{(2n)!}. \quad \text{(A32)}$$

The central moment notation is used since, by (A4), one can show that this is valid for any spectrum that is symmetric about its mean.

REFERENCES

Dazhang, T., and R. E. Passarelli, 1983: A new method for inferring raindrop size distributions and verticle incidence Doppler spectra. *Preprints 21st Conf. on Radar Meteorology,* Edmonton, Canada, Amer. Meteor. Soc., 198–205.

Miller, K. S., and M. M. Rochwarger, 1972: A covariance approach to spectral moment estimation. *IEEE Trans. Inform. Theory,* **IT-18,** 588–596.

Oppenheim, A. V., and R. W. Schafer, 1975: *Digital Signal Processing.* Prentice-Hall, 585 pp.

Passarelli, R. E., 1983: Parametric estimation of Doppler spectral moments: An alternative ground clutter rejection technique. *J. Climate Appl. Meteor.,* **22,** 851–858.

——, and A. D. Siggia, 1981: The autocorrelation function and Doppler spectral moments: Geometric and asymptotic interpretations. *Preprints 20th Conf. on Radar Meteorology,* Boston, Amer. Meteor. Soc., 301–307.

Rummler, W. E., 1968: Introduction of a New Estimator for Velocity Spectral Parameters. Tech Memo MM-68-4121-5, Bell Telephone Labs., 24 pp.

Siggia, A. D., 1981: A real-time Doppler spectrum analyzer. *Preprints 20th Conf. on Radar Meteorology,* Boston, Amer. Meteor. Soc., 222–227.

Sirmans, D., and B. Bumgarner, 1975: Numerical comparison of five mean frequency estimators. *J. Appl. Meteor.,* **14,** 991–1003.

Srivastava, R. C., A. R. Jameson and P. H. Hildebrand, 1979: Time-domain computation of mean and variance of Doppler spectra. *J. Appl. Meteor.,* **18,** 189–194.

Strauch, R. G., R. A. Kropfli, W. B. Sweezy, W. R. Moninger and R. W. Lee, 1978: Improved Doppler velocity estimates by the poly-pulse-pair method. *Preprints 18th Conf. on Radar Meteorology,* Atlanta, Amer. Meteor. Soc., 376–380.

Zrnic', D. S., 1979: Estimation of spectral moments for weather echoes. *IEEE Trans. Geosci. Elec.,* **GE-17,** 113–128.